Sato et al. Zoological Studies (2015) 54:18
DOI 10.1186/s40555-014-0098-z

Zoological Studies
a SpringerOpen Journal

RESEARCH Open Access

Spatial and temporal changes in zooplankton abundance, biovolume, and size spectra in the neighboring waters of Japan: analyses using an optical plankton counter

Kaede Sato[1], Kohei Matsuno[2], Daichi Arima[1], Yoshiyuki Abe[1] and Atsushi Yamaguchi[1*]

Abstract

Background: An optical plankton counter (OPC) was used to examine spatial and temporal changes in the zooplankton size spectra in the neighboring waters of Japan from May to August 2011.

Results: Based on the zooplankton biovolume of equivalent spherical diameter (ESD) in 45 bins for every 0.1 mm between 0.5 and 5.0 mm, a Bray-Curtis cluster analysis classified the zooplankton communities into six groups. The geographical distribution of each group varied from each of the others. Groups with a dominance of 4 to 5 mm ESD were observed in northern marginal seas (northern Japan Sea and Okhotsk Sea), while the least biovolume with a dominance of a small-size class (0.5 to 1 mm) was observed for the Kuroshio extension. Temporal changes were observed along the 155° E line, i.e., a high biovolume group dominated by 2 to 3 mm ESD during May shifted to other size spectra groups during July to August. These temporal changes were caused by the seasonal vertical descent of dominant large *Neocalanus* copepods during July to August. As a specific characteristic of the normalized biomass size spectra (NBSS), the slope of NBSS was moderate (−0.90) for the *Neocalanus* dominant spring group but was at −1.11 to −1.24 for the other groups. Theoretically, the slope of the NBSS of the stable marine ecosystem is known to settle at approximately −1.

Conclusions: Based on the analysis by OPC, zooplankton size spectra in the neighboring waters of Japan were separated into six groups. Most groups had −1.11 to −1.24 NBSS slopes, which were slightly higher than the theoretical value (−1). However, one group had a moderate slope of NBSS (−0.90) caused by the dominance of large *Neocalanus* copepods.

Keywords: NBSS; *Neocalanus*; OPC; Zooplankton

Background

From the perspective of fisheries, mesozooplankton is an important food source for pelagic fish and larvae. The size of the mesozooplankton determines the bioenergetics of fish (Sheldon et al. 1977) and affects the growth and mortality rates of fish larvae (Van der Meeren and Næss 1993). From the perspective of oceanography, the size of the mesozooplankton is also important. In an oceanic region (>200 m depth, 92% of ocean area), mesozooplankton transport particulate organic matter vertically from the surface to deeper layers (Longhurst 1991; Boyd and Newton 1999). The activity of this process, termed "biological pump," is known to be correlated with the size of dominant mesozooplankton in the epipelagic layer (Michaels and Silver 1988; Ducklow et al. 2001). Thus, information on the size spectra of mesozooplankton community is important from the viewpoint of both fisheries and oceanography.

The size spectra of the mesozooplankton community were evaluated using NBSS (cf. Marcolin et al. 2013). The size of the mesozooplankton was accurately quantified

* Correspondence: a-yama@fish.hokudai.ac.jp
[1]Laboratory of Marine Biology, Graduate School of Fisheries Science, Hokkaido University, 3-1-1 Minatomachi, Hakodate, Hokkaido 041-8611, Japan
Full list of author information is available at the end of the article

using an optical plankton counter (OPC, Herman 1988). Recently, spatial and temporal changes in the size spectra of worldwide ocean mesozooplankton were evaluated by NBSS obtained using OPC measurements (cf. Huntley et al. 1995; Piontkovski et al. 1995; Zhou and Huntley 1997; Herman and Harvey 2006; Kimmel et al. 2006). The slope of NBSS is an index of bottom-up or top-down control of the marine ecosystem (Zhou 2006). In a nutrient-rich high productivity ecosystem, dominance of small-sized mesozooplankton induced a high intercept and slope of NBSS (bottom-up). However, high predation on the smaller size class may induce a low intercept and slope of NBSS (top-down) (Moore and Suthers 2006). Visual predators such as fish typically remove large particles, which act to steepen the slope and maintain the intercept (Suthers et al. 2006). Thus, information on spatial and temporal changes in mesozooplankton NBSS is highly valuable for evaluating structures of the marine ecosystem (cf. García-Comas et al. 2014).

The neighboring waters of Japan include the subarctic, transitional, and subtropical Western North Pacific and their adjacent seas: Okhotsk Sea, Japan Sea, and East China Sea. The oceanographic characteristics of these oceans vary greatly from each other. Various studies have been previously performed on mesozooplankton abundance, biomass, and community structure in these oceans. For example, studies were performed in the subarctic and transitional Western North Pacific (Odate 1994; Chiba et al. 2006, 2008, 2009), the subtropical Western North Pacific (Nakata et al. 2001; Nakata and Koyama 2003), and the Japan Sea (Hirota and Hasegawa 1999; Iguchi 2004). Based on these studies, regional, seasonal, and annual changes in mesozooplankton abundance, biomass, and community structure were evaluated. However, little information is available for their size spectra, and few attempts have been made regarding NBSS analysis. Because the NBSS of zooplankton connects phytoplankton with fisheries biomass, providing spatial and temporal change patterns of NBSS in this region will be valuable.

In the present study, spatial and temporal changes in the mesozooplankton size spectra in the neighboring waters of Japan (subarctic, transitional, and subtropical Western North Pacific and their adjacent seas: Okhotsk Sea, Japan Sea, and East China Sea) were evaluated using OPC measurements of net mesozooplankton samples collected by the same methods between May and August 2011. For all of the OPC data, NBSS analyses were performed and compared with the NBSS reported from various worldwide oceans. These comparisons revealed spatial and temporal changes in the size spectra of mesozooplankton in the neighboring waters of Japan; additionally, their characteristics were evaluated.

Methods

Field sampling

Mesozooplankton samplings were obtained on board the T/S *Oshoro-Maru* along the 155° E line (38° to 44° N) in the Western North Pacific from May 16 to 20, in the Okhotsk Sea from June 10 to 11, in the Japan Sea from June 8 to 24, in the East China Sea from July 1 to 9, in the subtropical Western North Pacific from July 11 to 12, and along the 155° E line (38° to 44° N) in the Western North Pacific from July 27 to August 2, 2011. The total number of stations was 78 (Figure 1). Samples were collected via the vertical hauls of a NORPAC net (mouth diameter 45 cm, mesh size 335 μm, Motoda 1957) from 150 m to the surface during the day and/or night. At stations where the depth was shallower than 150 m, vertical tows from 5 m above the bottom were performed. The volume of water filtered through the net was estimated from a reading of the flowmeter (Rigosha & Co., Ltd., Saitama, Japan) mounted on the net ring. The collected samples were immediately fixed with 5% borax-buffered formalin on board the ship. At each station, temperature and salinity were measured using a CTD system (Sea-Bird SBE 911 Plus, Sea-Bird Electronics, Bellevue, WA, USA). Because sampling depths varied from station to station (from 0 to 30 to 0 to 150 m), we applied temperature and salinity data at the euphotic zone (0 to 30 m) to evaluate their spatial and temporal changes (Figure 2).

OPC measurements

At the land laboratory, the mesozooplankton samples were divided into half-aliquots using a Motoda box splitter (Motoda 1959). For each half-aliquot, the zooplankton were filtered using a 100-μm mesh under low vacuum, and the wet mass was measured using an electronic microbalance with a precision of 10 mg. The remaining 1/2 sub-samples were used for OPC (Model OPC-1 L: Focal Technologies Corp., Dartmouth, NS, Canada) measurements using the flow-through system (CT&C Co. Ltd., Tokyo, Japan). OPC measurements were made at a low flow rate (*ca.* 10 L min^{-1}) and low particle density (<10 counts s^{-1}) without staining (Yokoi et al. 2008).

Abundance and biovolume

The abundance per cubic meter (N: ind. m^{-3}) for each of the 4,096 ESD size categories was calculated from the following equation:

$$N = \frac{n}{s \times F}$$

where n is the number of particles (=zooplankton ind.), s is the split factor of each sample, and F is the filtered volume of the net (m^3). The biovolume of the zooplankton community at 4,096 size categories was calculated from the ESD data, and the biovolume (mm^3 m^{-3}) was calculated by

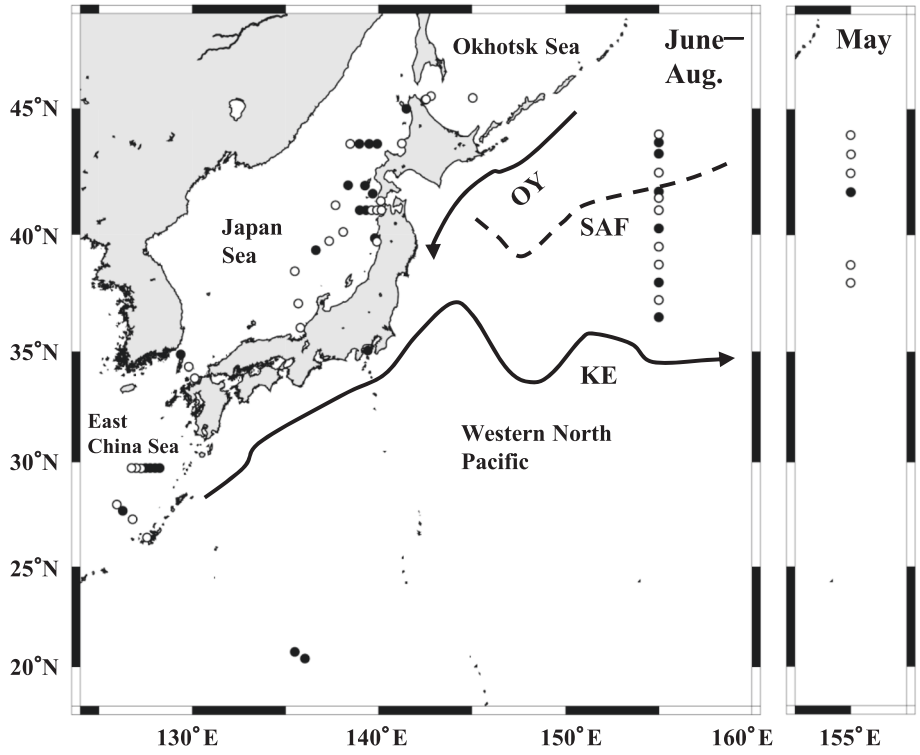

Figure 1 Location of sampling stations in the Western North Pacific and their adjacent seas. From May 16 to 20 (right panel) and June 8 to August 2 (left panel) 2011. Open and solid symbols denote stations where sampling was performed during the day and night, respectively. Approximate positions of OY: Oyashio, KE: Kuroshio Extension and SAF: Subarctic Front are superimposed (cf. Yasuda 2003). Samplings were conducted during the following periods: Western North Pacific along 155° E line (38° to 44°N) from May 16 to 20, Okhotsk Sea from June 10 to 11, Japan Sea from June 8 to 24, East China Sea from July 1 to 9, subtropical Western North Pacific from July 11 to 12 and along the 155° E line (38° to 44° N), in the Western North Pacific from July 27 to August 2, 2011.

multiplying N and volume (mm^3 $ind.^{-1}$) derived from ESD. Analyses on the mesozooplankton biovolume were performed with separation of six size classes (0 to 1, 1 to 2, 2 to 3, 3 to 4, 4 to 5, and >5 mm ESD). Day and night samplings accounted for 44 and 34 stations of all sampling stations, respectively (Figure 1). Day-night comparisons of the entire zooplankton abundance and biomass based on the whole sampling area showed no significant differences (U-test, abundance: $p = 0.567$, biomass: $p = 0.945$); thus, no day-night conversion for abundance or biomass was necessary.

Cluster analysis

To evaluate spatial and temporal changes in the size spectra of the zooplankton biovolume, cluster analysis was performed. Prior to the analysis, the biovolume data on 1,744 categories between 0.5 and 5.0 mm ESD were binned into 45 size classes at 0.1 mm ESD intervals (0.5 to 0.6, 0.6 to 0.7,..., 4.9 to 5.0 mm). Based on these biovolume data, similarities between the samples were evaluated using Bray-Curtis methods. To group the samples, similarity indices were coupled with hierarchical agglomerative clustering using a complete linkage method (Unweighted Pair Group Method using Arithmetic mean, UPGMA; Field et al. 1982). Non-metric multidimensional scaling (NMDS) ordination was performed to delineate the sample groups on a two-dimensional map (Field et al. 1982). To clarify which environmental parameters (latitude, longitude, integrated mean temperature and salinity at 0 to 30 m) exhibited significant relationships with the zooplankton sample groups, multiple regressions ($Y = aX_1 + bX_2 + c$, where Y is the environmental variable, X_1 and X_2 are axes 1 and 2 of NMDS, and a, b, and c are constants, respectively) were made using StatView (SAS Institute Inc., Cary, NC, USA).

Normalized biomass size spectra

From the OPC data, NBSS was calculated following Zhou (2006). First, zooplankton biovolume ($\bar{B}$: mm^3 m^{-3} [=μm^3 L^{-1}]) was averaged for every 100 μm ESD size class. To calculate the X-axis of NBSS (X: $\log_{10}$ zooplankton biovolume [mm^3 $ind.^{-1}$]), $\bar{B}$ was divided by the abundance of each size class (ind. m^{-3}) and converted to a common logarithm. To calculate the Y-axis of NBSS

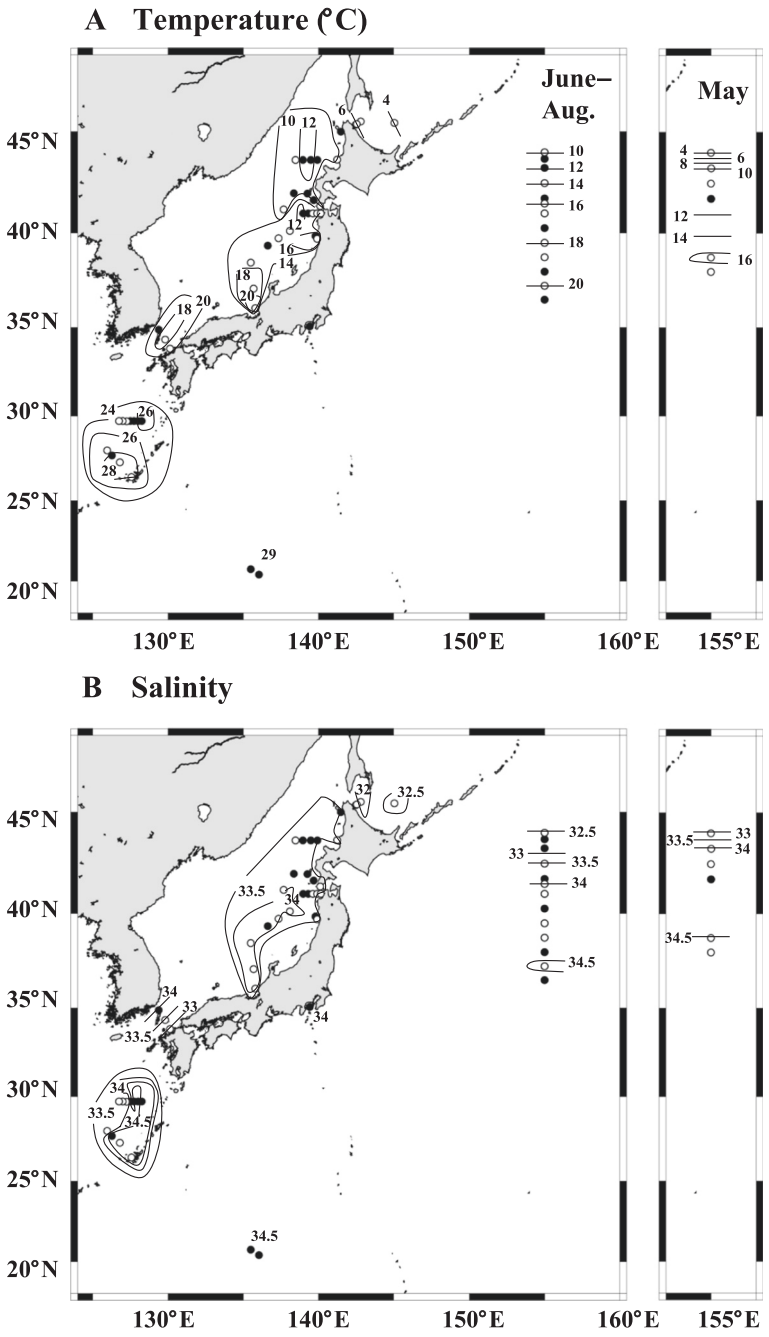

Figure 2 Horizontal distribution of the integrated mean temperature (A) and salinity (B). At 0 to 30 m in the Western North Pacific and their adjacent seas from May 16 to 20 (right panels) and June 8 to August 2 (left panels) 2011. Open and solid symbols denote stations where sampling was performed during the day and night, respectively.

(Y: $\log_{10}$ zooplankton biovolume [$mm^3\ m^{-3}$]/Δbiovolume [mm^3]), $\bar{B}$ was divided by the interval of biovolume (Δbiovolume [mm^3]) and converted to a common logarithm. Based on these data, the NBSS liner model ($Y = aX + b$) was calculated, where a and b are the slope and intercept of NBSS, respectively.

Statistical analysis

Based on the mesozooplankton groups clustered based on their size spectra, inter-group differences in the zooplankton data (abundance, biovolume, and slope of NBSS) were tested using one-way analysis of variance (ANOVA) and Fisher's protected least-squares difference (PLSD)

method. To determine the factors that govern the slope of NBSS, an analysis of covariance (ANCOVA) was performed using StatView, in which the intercept of NBSS and zooplankton group as independent variables.

Results

Hydrography

Throughout the entire sampling area and period, the integrated mean temperature at 0 to 30 m in the water column of each station ranged from 3.8 to 29.4°C (Figure 2A). Integrated mean temperatures were lower in the Okhotsk Sea and higher at the southern low-latitude station. With the temporal change between May and June to August, the temperature along the 155° E line in the Western North Pacific increased *ca.* 4°C within the same latitude from June to August. Integrated mean salinity ranged from 32.2 to 34.7 (Figure 2B) and showed a similar pattern to that of the integrated mean temperature and thus was lower in the Okhotsk Sea and higher in the southern low-latitude stations. Temporal changes in salinity along 155° E between May and June to August were not marked; this was comparable to the case of integrated mean temperature (Figure 2B).

OPC calibration

Comparison between OPC-derived wet mass (Y: mm^3 m^{-3}) and measured wet mass (X: mg m^{-3}) showed a highly significant correlation ($Y = 0.950X$, $r^2 = 0.691$, $p < 0.0001$, Figure 3). As an exception, one station (41° N, 155° E in 25 July) returned substantially higher values of direct measurement mass (marked with an open symbol in Figure 3). From microscopic observation, dominance of fragments of jellyfish and doliolids was the cause of the sample variation. We excluded the data of this station from the following analysis.

Zooplankton abundance, biovolume, and community

Zooplankton abundance ranged from 16.8 to 1,076 ind. m^{-3} and showed no clear spatial and temporal change pattern (Figure 4A). Zooplankton biovolume ranged from 2.24 to 1,007 mm^3 m^{-3} and was higher for the northern stations, particularly in the northern Japan Sea and north of the 155° E line (Figure 4B). Regarding temporal change, biovolume along the 155° E line was higher in May compared to June to August, with a factor of 1.4 to 9.8 times at the same latitude.

Based on the biovolume data of 45 size classes binned at every 0.1 mm, zooplankton communities were classified into six groups (A, B1, B2, B3, C, and D) using cluster analysis at 42% dissimilarities (Figure 5A). Each group contained 7 to 20 stations. Hydrographic variables showing significant relationships on the NMDS ordination were integrated mean temperature and integrated mean salinity at 0 to 30 m water column; these variables accounted for 18% and 15% of the changes, respectively.

Total abundance also significantly varied according to group and was the least for group D, followed by group A and was the highest for group B3 (Table 1). Total abundance was dominated by the 0.5 to 1 mm ESD size class for all groups. For the 1 to 2, 2 to 3, and 3 to 4 mm ESD size classes, the highest abundance was observed for group C. Moreover, the 4 to 5 mm ESD size class was the highest for group B1. Thus, the highest abundance group varied with size classes (Table 1).

For the total biovolume, the common group order was the least for group D followed by group A as observed for all size classes (Table 1, Figure 5C). The highest zooplankton biovolume was observed for group C; this was due to the dominance of biovolume at the 2 to 3 mm ESD size class (Figure 5C). Within the size class, group B3 was the highest in the 0.5 to 1 mm size class, while group B1 was the highest in the 4 to 5 mm size class. For the other size classes (1 to 2, 2 to 3, and 3 to 4 mm), group C was the highest biovolume group (Table 1).

The horizontal and temporal distribution of each group varied from those of the others (Figure 6). Groups A, B2, and B3 occurred in a broader region: Japan Sea, Western North Pacific, and East China Sea and had no geographical pattern. However, the horizontal distribution of groups B1, C, and D showed a clear geographical pattern. Group B1 was dominated by a large 4 to 5 mm ESD size class and was found in the Northern Japan Sea, Okhotsk Sea, and subarctic Western North Pacific. Group

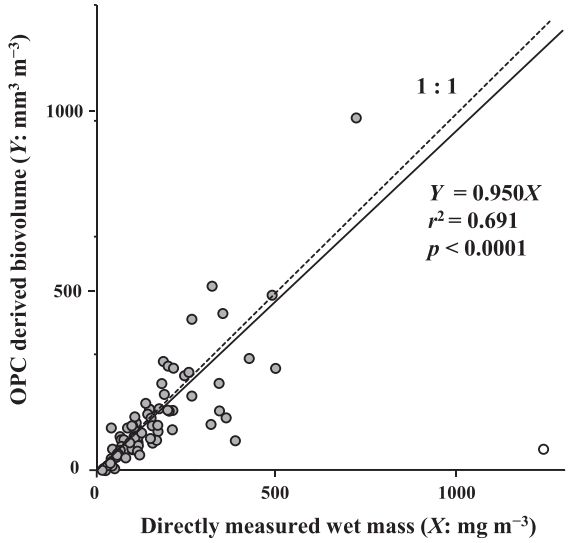

Figure 3 Comparison between OPC-derived biovolume and directly measured wet mass of whole samples. The long-dashed line indicates position 1:1. One datum at an anomalously high value of directly measured wet mass indicated by an open symbol was omitted from the following analysis.

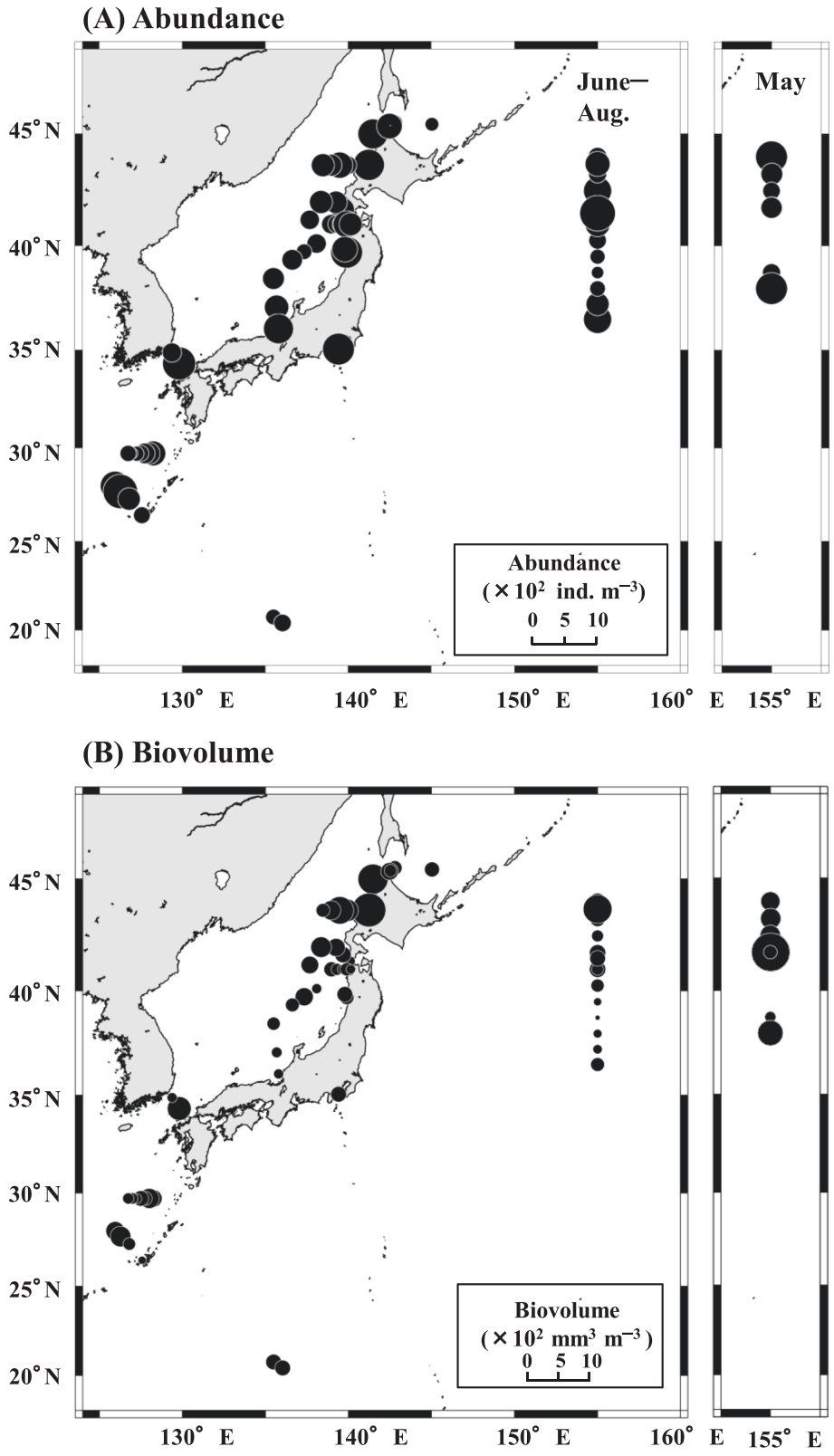

Figure 4 Horizontal distribution of abundance (A) and biovolume (B) of mesozooplankton in the Western North Pacific and adjacent seas. From May 16 to 20 (right panels) and June 8 to August 2, 2011 (left panels).

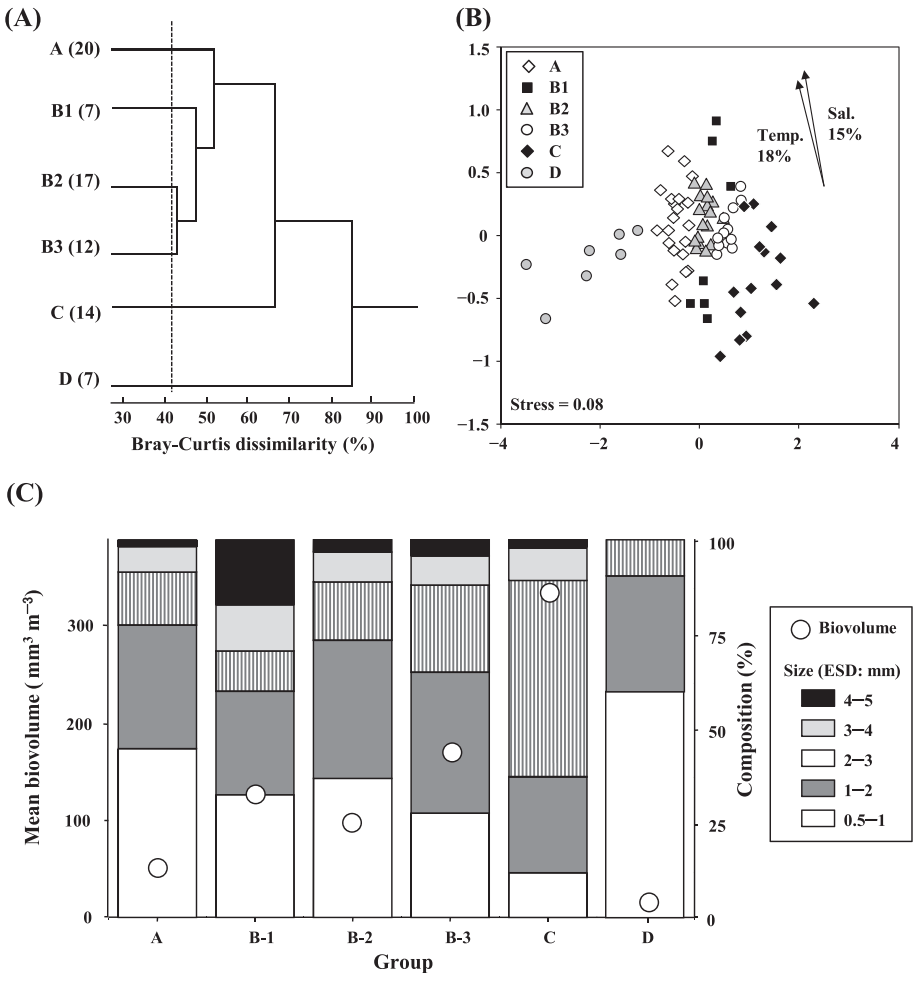

Figure 5 Results of cluster analysis based on mesozooplankton biovolume size spectra. In the Western North Pacific and adjacent seas from May and June to August 2011. **(A)** Six groups (A, B1, B2, B3, C, and D) were identified from Bray-Curtis dissimilarity connected with UPGMA. Numbers in parentheses indicate the number of stations contained in each group. **(B)** NMDS plots of each group. For correlation analyses with environmental parameters (temperature, salinity, latitude, and longitude), temperature and salinity showed a significant correlation (percentage indicates the coefficients of determination, r^2). **(C)** Mean biovolume and size composition (ESD, mm) of each group.

C, which was characterized by the highest biovolume and dominance of the 2 to 3 mm size class, occurred along the 155° E line during May and in the northern Japan Sea, Okhotsk Sea, and subarctic Western North Pacific from June to August. Group D, which was characterized by the least biovolume and was dominated by a small-sized 0.5 to 1 mm size class, was found at lower latitudes of the 155° E line (Kuroshio extension) (Figure 6).

NBSS

Results of the mean NBSS based on the complete data of each group are shown in Figure 7. For group C, the marked peak value on the *X*-axis ($\log_{10}$ zooplankton biovolume [mm^3 $ind.^{-1}$]) was observed at approximately 0.7; this corresponded with a 2 to 3 mm ESD size class and consisted of the copepodid stage 5 of the large copepod *Neocalanus* spp. (Figure 7). Significant inter-group differences were observed for the slope (*a*) and intercept (*b*) of NBSS (Table 1). The moderate slope (–0.90) of group C was significantly different from those of other groups (–1.11 ~ –1.24) (ANCOVA, $p < 0.001$, Table 2). For the intercept, the least was found for group D, while the highest was found for group C; the order of the intercept of each group corresponded to the order of total zooplankton biovolume (Table 1). From the ANCOVA analysis, there was no interaction between group and intercept, but significant relationships between slope and group were found ($p < 0.0001$, Table 2).

Discussion

OPC measurements

There have been several studies on OPC measurements for zooplankton in the western North Pacific. Table 3

Table 1 Comparison of zooplankton abundance, biovolume, and slopes (*a*) and (*b*) of NBSS ($Y = aX + b$) of each group

	Group						One-way ANOVA	Fisher's PLSD				
Parameter	A(20)	B1(7)	B2(17)	B3(12)	C(14)	D(7)						
Abundance (inds. m^{-3})												
Total	331	503	476	528	469	101	**	D	A	C	B2	B1 **B3**
0.25 to 1 mm	315	465	441	473	387	98	**	D	**A**	**C**	**B2**	**B1** **B3**
1 to 2 mm	15.1	34.0	32.3	48.5	52.3	2.9	***	D	A	B1	B2	**B3** **C**
2 to 3 mm	1.1	2.1	2.4	6.2	28.3	0.1	***	D	A	B1	B2	B3 **C**
3 to 4 mm	0.2	0.8	0.4	0.7	1.5	0.0	**	D	A	B2	B3	B1 **C**
4 to 5 mm	0.0	0.5	0.1	0.2	0.2	0.0	***	D	A	B2	C	B3 **B1**
Biovolume (mm^3m^{-3})												
Total	57.0 ± 13.8	135.1 ± 34.1	106.7 ± 39.3	179.6 ± 44.7	348.7 ± 229.1	10.7 ± 7.5	***	D	A	B2	B1	B3 **C**
0.25 to 1 mm	25.7 ± 11.9	43.9 ± 30.9	39.3 ± 13.9	49.6 ± 21.5	41.3 ± 27.5	6.5 ± 4.7	***	D	A	**B2**	**C**	**B1** **B3**
1 to 2 mm	18.6 ± 7.1	37.0 ± 17.3	39.0 ± 9.6	66.9 ± 16.9	88.7 ± 46.2	3.3 ± 2.2	***	D	A	B1	B2	B3 **C**
2 to 3 mm	7.7 ± 4.1	14.5 ± 12.8	16.5 ± 6.1	41.5 ± 12.1	181.4 ± 160.9	1.0 ± 0.9	***	D	A	B1	B2	B3 **C**
3 to 4 mm	3.9 ± 4.1	16.5 ± 10.9	8.5 ± 7.5	13.9 ± 9.1	30.5 ± 42.7	0	**	D	A	B2	B3	B1 **C**
4 to 5 mm	1.1 ± 1.6	23.3 ± 24.1	3.5 ± 4.3	7.7 ± 9.9	6.7 ± 9.0	0	***	D	A	B2	C	B3 **B1**
NBSS												
Slope (*a*)	−1.18 ± 0.14	−1.11 ± 0.16	−119 ± 0.94	−1.16 ± 0.94	−0.90 ± 0.16	−1.24 ± 0.11	**	D	B2	A	B3	B1 **C**
Intercept (*b*)	−0.23 ± 0.28	−0.06 ± 0.32	−0.04 ± 0.16	0.09 ± 0.27	0.29 ± 0.29	−0.65 ± 0.29	***	D	A	B1	B2	B3 **C**

Identified by Q-mode analysis (cf. Figure 5A) in the Western Pacific and their adjacent seas during May and June to August 2011. Differences between the group were tested by one-way ANOVA and *post hoc* test by Fisher's PLSD. Groups with bold letters indicate that the groups are significantly greater than the other groups ($p < 0.05$). Values are mean ± s.d. Numbers in the parentheses are the numbers of stations belonging to each group. **$p < 0.01$, ***$p < 0.0001$.

summarizes regressions between the OPC-derived mass and directly measured mass, ranges of zooplankton abundance, and biovolume from previous studies. The OPC-derived masses were 1.05 to 1.18 times the directly measured mass in previous studies (Yokoi et al. 2008; Matsuno and Yamaguchi 2010; Fukuda et al. 2012). In this study, the zooplankton biovolume estimated by OPC was 0.95 times the directly measured mass (Figure 3). This factor is slightly smaller than the previously reported values, but all these values (0.95 to 1.18) corresponded well at nearly 1:1. In the present study, a substantial underestimation of the OPC biovolume was caused by fragments of jellyfish and doliolids at one station (41° N, 155° E on 29 July). Regarding dominance of doliolids and gelatinous zooplankton in the Western North Pacific, Yokoi et al. (2008) reported that their dominance was observed at locations of thermocline-developed stations in the transitional domain. This condition may also have been present at 41° N, 155° E on July 29 of this study.

Based on this same method (OPC measurement of net samples), zooplankton abundance and biovolume in the Western North Pacific were reported ranging from 128 to 580 ind. m^{-3} and 96 to 880 mm^3 m^{-3}, respectively (Yokoi et al. 2008; Matsuno and Yamaguchi 2010; Fukuda et al. 2012). Both the zooplankton abundance (16.8 to 1,076 ind. m^{-3}) and biovolume (2.24 to 1,007 mm^3 m^{-3}) in this study fell in these ranges. This was shown by previous studies based on 0 to 150 m samplings obtained offshore in the North Pacific; this study included neritic to oceanic regions of the North Pacific and marginal seas, and sampling depths varied with each station (the shallowest station was 0 to 30 m sampling). These discrepancies in methodology (region and sampling depth) between previous studies and this study might have induced the extension of the range of abundance and biovolume data in this study.

Spatial changes

For spatial changes in zooplankton, the higher biovolume at high latitudes (Figure 4B) and horizontal distributions of groups B1, C, and D showed distinct geographical patterns (Figure 6).

Group B1 was observed only in areas north of the Japan Sea, in the Okhotsk Sea, and at the subarctic region along the 155° E line in the Western North Pacific (Figure 6). For zooplankton biomass in the Japan Sea, the southern part was reported to be less than that found in the north and was similar to that of the Kuroshio region of the Western North Pacific (Hirota and Hasegawa 1999; Iguchi 2004). Common to this study, the zooplankton biovolume in the Japan Sea was higher in the northern area (Figure 4B). In the northern Japan Sea, where the surface

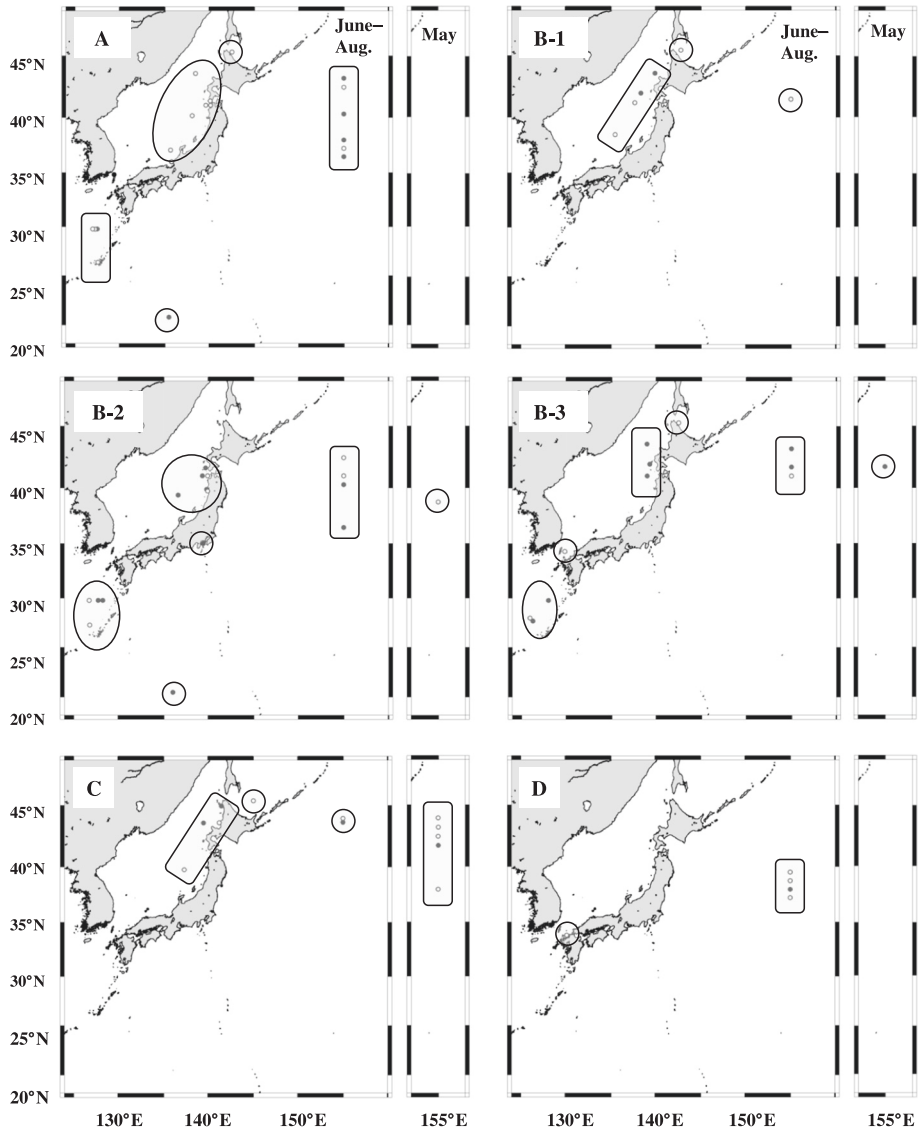

Figure 6 Horizontal distribution of six groups (A, B1, B2, B3, C, and D) identified from cluster analysis on mesozooplankton biovolume size spectra (cf. Figure 5A). In the Western North Pacific and adjacent seas from May and June to August 2011. Open and solid symbols denote day and night samples, respectively. The geographical ranges of each group are marked with boxes and circles.

temperature is low, the large-sized cold-water species, i.e., chaetognath *Parasagitta elegans*, amphipod *Themisto japonica* and euphausiid *Euphausia pacifica* are known to perform diel vertical migration and distribute on the surface at night (Ikeda et al. 1992; Iguchi et al. 1993; Terazaki 1993). The proportion of 4 to 5 mm ESD in group B1 was much higher than that in the other groups (Figure 5C). This size range (4 to 5 mm) exceeded the size of copepods (the size of the largest copepods in this region: *Neocalanus* spp. C5 is 2 to 3 mm ESD, Yokoi et al. 2008) and was considered caused by macrozooplankton such as amphipods, euphausiids, and chaetognaths. These taxa frequently occurred for samples belonging to group B1. The dominance of large-sized chaetognath *P. elegans* and amphipod *Themisto pacifica* was also reported for the Okhotsk Sea (Volkov 2008). Thus, group B1 was only observed for the northern area of the Japan Sea, Okhotsk Sea, and subarctic Western North Pacific, which were characterized by a higher proportion of the large 4 to 5 mm ESD size class consisting of macrozooplankton.

In contrast, the horizontal distribution of group D was only observed in the Kuroshio extension from June to August (Figure 6). Group D was characterized by the least biovolume and dominance of the small-size class (0.5 to 1 mm ESD) (Figure 5C). From microscopic observation, the samples belonging to group D were dominated

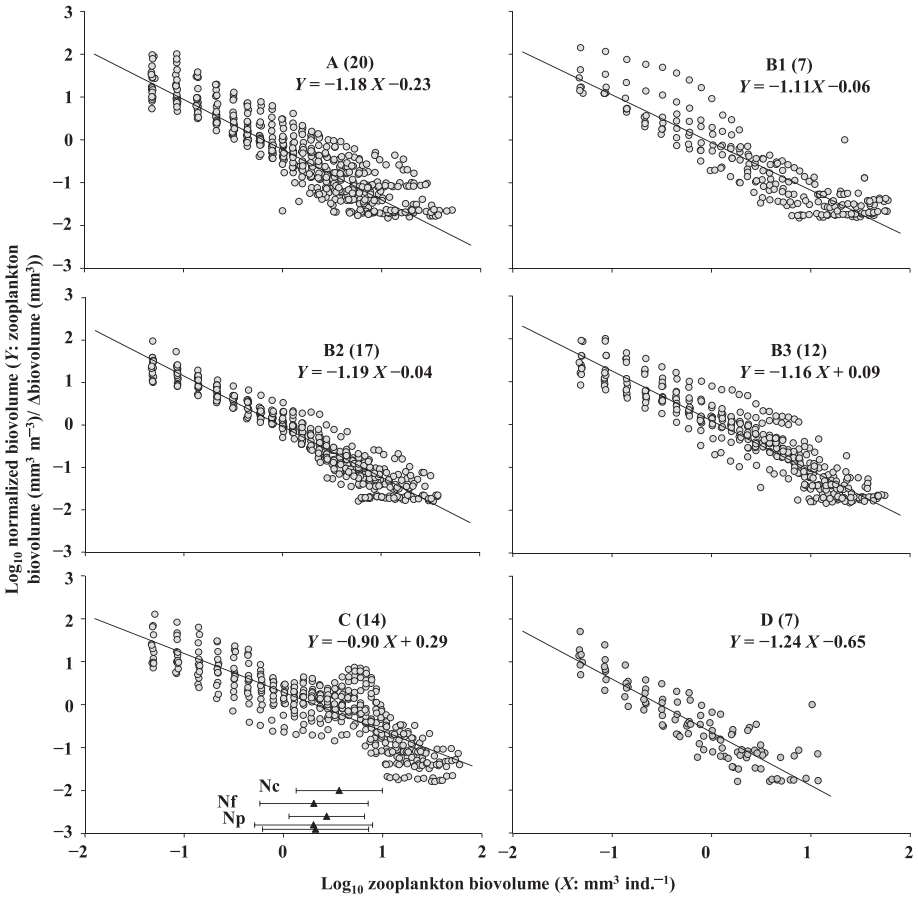

Figure 7 Mean NBSS of six groups (A, B-1, B-2, B-3, C and D) identified from cluster analysis on mesozooplankton biovolume size spectra (cf. Figure 5A). In the Western North Pacific and adjacent seas during May and June to August 2011. Numbers in parentheses indicate the number of stations belonging to each group. The mean and standard deviations of copepodid five stages of *Neocalanus* copepods (Nc, *Neocalanus cristatus*; Nf, *N. flemingeri*; and Np, *N. plumchrus*, Yamaguchi et al. 2014) are shown in panel for group **C**.

by small-sized copepods, e.g., *Paracalanus parvus* and poecilostomatoida. Hydrography of group D was also marked, and all of the stations showed high salinity (near 34.0, Figure 8), which is characteristic of the Kuroshio extension (Yasuda 2003). From the NMDS plot (Figure 5B), the direction of the two arrows indicates that groups A, B1, and C showed euryhaline and eurytherm, while the others (B2, B3, and D) were restricted, occurring in narrower ranges of temperature and salinity. These findings suggested that the horizontal distribution of zooplankton was regulated by water mass formation. In the Kuroshio region, it is well known that in an oligotrophic ocean, zooplankton fauna is dominated by small-sized copepods such as *Paracalanus* spp. and poecilostomatoida (Nakata et al. 2001; Nakata and Koyama 2003; Hsieh et al. 2004).

Table 2 Result of the ANCOVA for the slope (*a*) of NBSS ($Y = aX + b$)

Parameter	*df*	SS	*F*-value	*p*-value
Intercept	1	0.052	3.451	NS
Group	5	0.645	8.629	***
Group × Intercept	5	0.111	1.477	NS
Error	66	0.972	-	-

With the intercept (*b*) of NBSS and zooplankton group (cf. Figure 5A) applied as independent variables. *d.f.*, degrees of freedom; SS, sum of squares. N.S., not significant. ***$p < 0.0001$.

However, same ocean latitudes were adjusted with the Kuroshio extension; the East China Sea, southern coast of Japan, and southern Japan Sea were not as oligotrophic as the Kuroshio extension region, and middle-sized copepods, such as *Calanus sinicus*, are known to dominate in zooplankton fauna (Hirakawa et al. 1995; Shimode et al. 2006; Hsiao et al. 2011). Due to the dominance of middle-sized copepods (*C. sinicus*) for these marginal seas, zooplankton size spectra in these regions were dispersed into groups A, B2, and B3 (Figure 6). Thus, it is difficult to identify specific characteristics in the horizontal distribution of these groups.

Table 3 Comparison on regressions between OPC derived mass and directly measured mass, ranges of abudance, and biovolume of mesozooplankton

Location (period)	Regression (n, r^2, p)	Abundance (ind. m^{-3})	Biovolume (mm^3 m^{-3})	References
35° to 44° N, 155° E	$Y = 1.05X + 0.05$	351.7 to 579.5	177.1 to 678.9[a]	Yokoi et al. (2008)
(May to June 1993 to 2004)	(234, 0.63, $p < 0.0001$)			
22° to 53° 30′ N 165° E/165° W	$Y = 116X$	226.3 to 430.9	190.7 to 523.3[a]	Matsuno and Yamaguchi (2010)
(June to August 2003 to 2006)	(96, 0.79, $p < 0.0001$)			
35° to 51° N, 180°	$Y = 1.176X$	128.0 to 562.0	96.0 to 880.0[a]	Fukuda et al (2012)
(June 1981 to 2000)	(351, 0.521, $p < 0.0001$)			
20° to 45° N, 126° to 155° E	$Y = 0.950X$	16.8 to 1,075.9	2.2 to 1,006.7	This study
(May to Aug. 2011)	(78, 0.691, $p < 0.0001$)			

Evaluated by OPC analyses in the North Pacific. For regressions, Y, biovolume in mm^{-3} and X, mg m^{-3}.
[a]Biovolume data were calculated from dry mass unit in the references.

Temporal changes

In the present study, two time samplings in May and July to August were performed along the 155° E line in the Western North Pacific. In May, group C, which is characterized by a high biovolume and dominance of the 2 to 3 mm ESD size class, dominated; however, this changed to other groups during July to August (Figure 6). The 2 to 3 mm ESD zooplankton in this region corresponded with the C5 stages of large copepods *Neocalanus* spp., and their importance has been reported in previous OPC studies (Yokoi et al. 2008; Matsuno and Yamaguchi 2010; Fukuda et al. 2012). Along the 155° E line, group C was dominated by the 2 to 3 mm ESD size class and was characterized by a high biovolume during May and at the northern stations from July to August.

Neocalanus spp. is known to perform seasonal vertical migration. C1 of *Neocalanus* spp. grow to C5 near the surface from mid-March to June, descend to deep layers from June to August, and subsequently molt to an adult in the deep layers (Kobari et al. 2003). The large copepod *Eucalanus bungii* also perform seasonal vertical migration and reproduce near the surface from April to May during phytoplankton bloom (Shoden et al. 2005). Consequently, the total zooplankton biomass in this region peaked during May due to the dominance of *Neocalanus* and *Eucalanus* spp. near the surface (Odate 1994). The high biovolume dominated by the 2 to 3 mm ESD size class in May along the 155°E line in this study was caused by the dominance of these large copepods near the surface layer. After the descent of these large copepods into the deep layer, the biovolume decreased and size spectra characteristics changed to different groups from July to August.

The high biomass dominated by late copepodid stages of large copepods is a characteristic of a limited period (1 to 2 months in and near May) in the subarctic North Pacific (Odate 1994). This high zooplankton biomass season was reported to vary inter-annually owing to the decadal climate regime shift (Chiba et al. 2006, 2008). Chiba et al. (2006) observed that the zooplankton peak season in spring varied by one month depending on the decadal climate changes. Although there was a slight change in timing, the specific characteristics caused by seasonal changes in the zooplankton biomass of the neighboring waters of Japan were at high biomass caused by the dominance of large-sized copepods near the surface layer during spring.

NBSS

The slope of NBSS is known to be an index of productivity, transfer efficiency, and predation in each marine ecosystem (Zhou 2006; Zhou et al. 2009). From the theoretical mean, the slope of NBSS of the stable marine ecosystem settled at approximately −1 (Sprules and Munawar 1986). The steep slope of NBSS indicated high productivity but low transfer efficiency to a higher trophic level. However, the moderate NBSS slope may be caused by low productivity and high energy-transfer efficiency (Sprules and Munawar 1986). In the present study, the slopes of NBSS were slightly higher than −1 for most of the groups, except for group C (Table 1). These findings suggest that most of the zooplankton communities in neighboring Japanese waters were characterized by a bottom-up marine ecosystem. The intercept of NBSS is a reflection of the amount of primary production (Zhou 2006; Marcolin et al. 2013). The high correlation between the intercept of NBSS and the total zooplankton biovolume of each group in this study may confirm this theory (Table 1).

The slopes of NBSS of the zooplankton community reported from various oceans are summarized in Table 4. As previously mentioned, the slope of NBSS is an index of productivity, transfer efficiency, and predation. However, the treated size range varied with the study and ranged from microzooplankton (0.025 to 4.0 mm, Napp

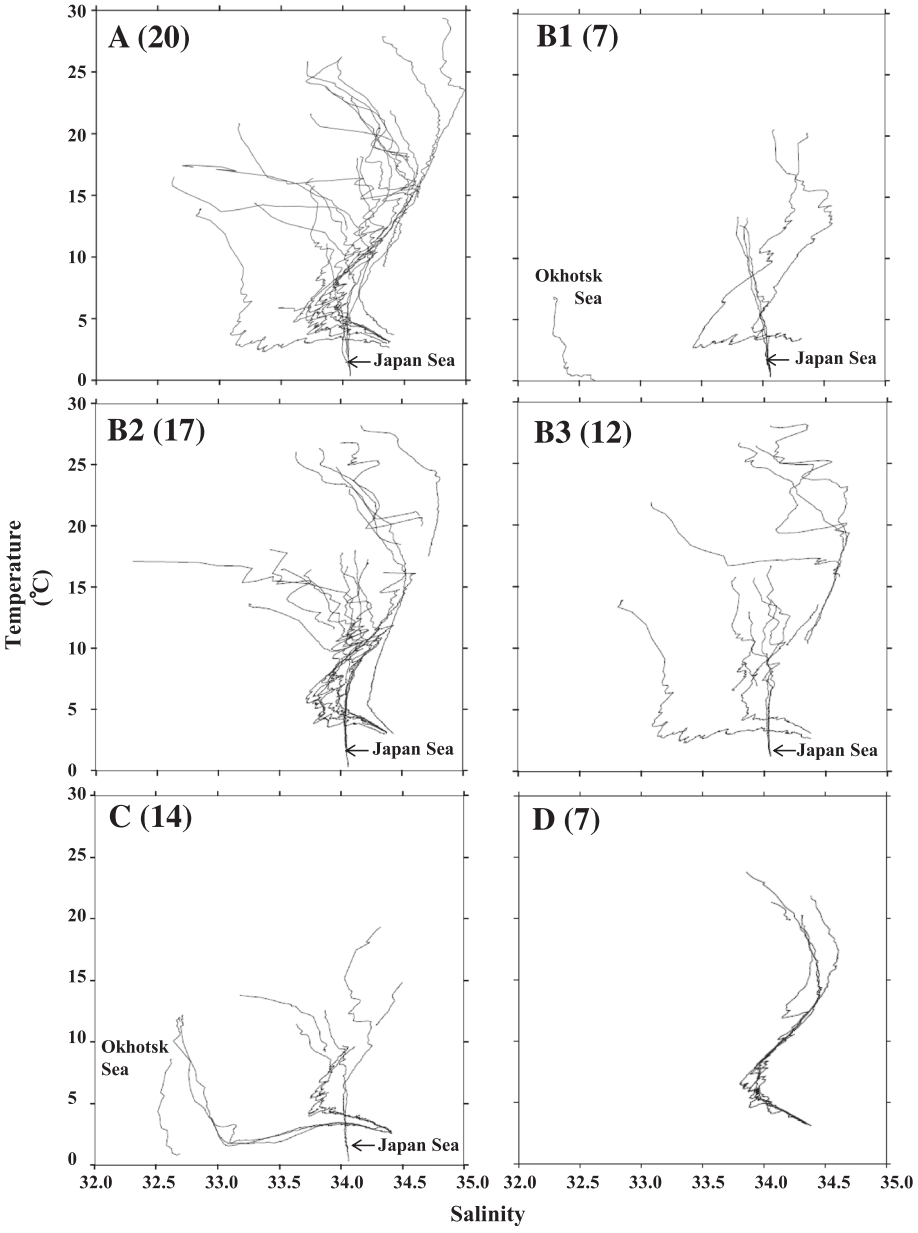

Figure 8 T-S diagrams of the six groups (A, B1, B2, B3, C, and D) identified from cluster analysis on mesozooplankton biovolume size spectra (cf. Figure 5A). In the Western North Pacific and adjacent seas from May and June to August 2011. To construct T-S diagrams, hydrographic data from 0 to 1,000 m were applied. The numbers in parentheses indicate the number of stations belonging to each group.

et al. 1993) to fish (20 to 1,200 mm, Macpherson et al. 2002). Thus, a careful, direct comparison of the NBSS slope is required. In the present study, specific characteristics of the NBSS slope include a moderate slope of group C (−0.90) caused by the dominance of C5 stages of large *Neocalanus* spp. (Figure 7). Along the 155° E line, group C during May varied with other groups from July to August; thus, the temporal changes were remarkable (Figure 6). A similar situation (alternation of NBSS slope by dominance of specific taxa) was reported for the dominance of barnacle larvae in the Chukchi Sea (Matsuno et al. 2012).

Conclusions

Through OPC analysis of zooplankton samples, zooplankton size spectra in the neighboring waters of Japan were separated into six groups. Most groups had −1.11 to −1.24 NBSS slopes, which were slightly higher than the theoretical value (−1). However, one group had moderate slope NBSS (−0.90) caused by the dominance of large

Table 4 Comparison of the slope (*a*) of NBSS ($Y = aX + b$) on the mesozooplankton community at various locations

Location/region	Unit	Size range (mm)	Slope	References
Chile, cold nutrient-rich conditions	Carbon	0.7 to 210	−0.44	Iriarte and González (2004)
Gulf of St. Lawrence (open water)	Biovolume	0.25 to 2	−0.47	Herman and Harvey (2006)
Barents Sea	Biovolume	0.25 to 14	−0.63	Basedow et al. (2010)
NW Mediterranean (protected area)	Wet weight	20 to 1,200	−0.65	Macpherson et al. (2002)
Bay of Biscay (oceanic stations)	Carbon	0.27 to 1.7	−0.71 to −0.64	Sourisseau and Carlotti (2006)
Tasman Sea	Biovolume	0.11 to 3.3	−0.69	Baird et al. (2008)
Unshant Tidal Front (stratified side/offshore)	Carbon	0.5 to 5	−0.73	Schultes et al. (2013)
Brazilian Continental Shelf (Oceanic Stations)	Biovolume	0.1 to 5	−0.86	Marcolin et al. (2013)
Chukchi Sea (less productive)	Biovolume	0.25 to 5	−0.86	Matsuno et al. (2012)
Gulf of St. Lawrence (estuary)	Biovolume	0.25 to 2	−0.90	Herman and Harvey (2006)
Western Antarctic Peninsula (fall)	Biovolume	0.25 to 14	−0.92	Zhou et al. (2009)
Chile-El Nino, oligotrophic conditions	Carbon	0.7 to 210	−0.93	(Iriarte and González 2004)
Coral Sea	Biovolume	0.11 to 3.3	−0.97	Baird et al. (2008)
Southwest Coral Sea	Wet weight	0.25 to 2.5	−1.00	Suthers et al. (2006)
Bay of Biscay (coastal stations)	Carbon	0.27 to 1.7	−1.05 to −0.91	Sourisseau and Carlotti (2006)
NW Mediterranean (unprotected area)	Wet weight	20 to 1,200	−1.04	Macpherson et al. (2002)
Scotia Sea (spring)	Carbon	Small phyto to large schyphomedusae	−1.09	Tarling et al. (2012)
North Iberian Shelf	Carbon	0.25 to 17	−1.11	Nogueira et al. (2004)
Chukchi Sea (more productive)	Biovolume	0.25 to 5	−1.11	Matsuno et al. (2012)
North Pacific Ocean	Carbon	0.18 to 4.0	−1.13	Rodriguez and Mullin (1986)
Northwest Atlantic Ocean	Carbon	0.07 to 8.0	−1.14	Quinones et al. (2003)
Ushant Tidal Front (mixed side/nearshore)	Carbon	0.5 to 5	−1.15	Schultes et al. (2013)
Brazilian Continental Shelf (Coastal Stations and Abrolhos Bank)	Biovolume	0.1 to 5	−1.25	Marcolin et al. (2013)
California Current	Carbon	0.2 to 3.3	−1.43	Huntley et al. (1995)
Ushant Tidal Front (mixed side/near)	Carbon	0.5 to 5	−1.76	Schultes et al. (2013)
Western Antarctic Peninsula (summer)	Biovolume	0.25 to 14	−1.8	Zhou et al. (2009)
Australian Estuary	Wet weight	0.25 to 1.6	−1.89	Moore and Suthers (2006)
California Bight	Biovolume	0.025 to 4.0	−2.30	Napp et al. (1993)
NW Pacific (group A)	Biovolume	0.50 to 5.00	−1.18	This study
NW Pacific (group B1)	Biovolume	0.50 to 5.00	−1.11	This study
NW Pacific (group B2)	Biovolume	0.50 to 5.00	−1.19	This study
NW Pacific (group B3)	Biovolume	0.50 to 5.00	−1.16	This study
NW Pacific (group C)	Biovolume	0.50 to 5.00	−0.90	This study
NW Pacific (group D)	Biovolume	0.50 to 5.00	−1.24	This study

Neocalanus copepods. Temporal changes in the slope of NBSS were observed from moderate slope (−0.90) in May back to high NBSS slope (−1.11 to −1.24) caused by a descent of *Neocalanus* copepods to deep layers from July to August. This temporal change in the NBSS slope was not caused by predator-prey interaction, but due to the seasonal vertical migration of dominant large-sized zooplankton species. This finding suggests that the ecology of dominant species (growth or seasonal vertical migration) also should be considered as a cause of temporal changes in NBSS slope.

Competing interests

The authors declare that they have no competing interests.

Authors' contributions

KS and AY wrote the manuscript. KM, DA, and YA participated in the design of the study and helped with OPC measurements. All authors read and approved the final manuscript.

Acknowledgements
We are grateful to the captain and crew of the T/S *Oshoro-Maru* for their help in our field sampling. This study was supported by a Grant-in-Aid for Scientific Research (A) 24248032 and a Grant-in-Aid for Scientific Research on Innovative Areas 24110005 from the Japan Society for the Promotion of Science (JSPS).

Author details
[1]Laboratory of Marine Biology, Graduate School of Fisheries Science, Hokkaido University, 3-1-1 Minatomachi, Hakodate, Hokkaido 041-8611, Japan. [2]Arctic Environmental Research Center, National Institute of Polar Research, 10-3 Midori-cho, Tachikawa, Tokyo 190-8518, Japan.

Received: 14 July 2014 Accepted: 25 December 2014
Published online: 16 January 2015

References

Baird ME, Timko PG, Middleton JH, Mullaney TJ, Cox DR, Suthers IM (2008) Biological properties across the Tasman Front off southeast Australia. Deep-Sea Res I 55:1438–1455

Basedow SL, Tande KS, Zhou M (2010) Biovolume spectrum theories applied: spatial patterns of trophic levels within a mesozooplankton community at the polar front. J Plank Res 32:1105–1119

Boyd PW, Newton PP (1999) Does planktonic community structure determine downward particulate organic carbon flux in different oceanic provinces? Deep-Sea Res I 46:63–91

Chiba S, Tadokoro K, Sugisaki H, Saino T (2006) Effects of decadal climate change on zooplankton over the last 50 years in the western subarctic North Pacific. Global Change Biol 12:907–920

Chiba S, Aita MN, Tadokoro K, Saino T, Sugisaki H, Nakata K (2008) From climate regime shifts to lower-trophic level phenology: synthesis of recent progress in retrospective studies of the western North Pacific. Prog Oceanogr 77:112–126

Chiba S, Sugisaki H, Nonaka M, Saino T (2009) Geographical shift of zooplankton communities and decadal dynamics of the Kuroshio-Oyashio currents in the western North Pacific. Global Change Biol 15:1846–1858

Ducklow HW, Steinberg DK, Buesseler KO (2001) Upper ocean carbon export and the biological pump. Oceanography 14:50–58

Field JG, Clarke KR, Warwick RM (1982) A practical strategy for analysing multispecies distribution patterns. Mar Ecol Prog Ser 8:37–52

Fukuda J, Yamaguchi A, Matsuno K, Imai I (2012) Interannual and latitudinal changes in zooplankton abundance, biomass and size composition along a central North Pacific transect during summer: analyses with an Optical Plankton Counter. Plank Benthos Res 7:64–74

García-Comas C, Chang C-Y, Ye L, Sastri AR, Lee Y-C, Gong G-C, Hsieh C-H (2014) Mesozooplankton size structure in response to environmental conditions in the East China Sea: how much does size spectra theory fit empirical data of a dynamic coastal area? Prog Oceanogr 121:141–157

Herman AW (1988) Simultaneous measurement of zooplankton and light attenuance with new optical plankton counter. Cont Shelf Res 8:205–221

Herman AW, Harvey M (2006) Application of normalized biomass size spectra to laser optical plankton counter net inter comparisons of zooplankton distributions. J Geophys Res 111:C05S05, doi:10.1029/2005JC002948

Hirakawa K, Kawano M, Nishihama S (1995) Seasonal variability in abundance and composition of zooplankton in the vicinity of the Tsushima Straits, southwestern Japan Sea. Bull Japan Sea Natl Fish Res Inst 45:25–38

Hirota Y, Hasegawa S (1999) The zooplankton biomass in the Sea of Japan. Fish Oceanogr 8:274–283

Hsiao S-H, Ka S, Fang T-H, Hwang J-S (2011) Zooplankton assemblages as indicators of seasonal changes in water masses in the boundary waters between the East China Sea and the Taiwan Strait. Hydrobiologia 666:317–330

Hsieh C-H, Chiu T-S, Shih C-T (2004) Copepod diversity and composition as indicators of intrusion of the Kuroshio Branch Current into the northern Taiwan Strait in Spring 2000. Zool Stud 43:393–403

Huntley ME, Zhou M, Nordhausen W (1995) Mesoscale distribution of zooplankton in the California Current in late spring, observed by optical plankton counter. J Mar Res 53:647–674

Iguchi N (2004) Spatial/temporal variations in zooplankton biomass and ecological characteristics of major species in the southern part of the Japan Sea: a review. Prog Oceanogr 61:213–225

Iguchi N, Ikeda T, Imamura A (1993) Growth and life cycle of a euphausiid crustacean (*Euphausia pacifica* HANSEN) in Toyama Bay, southern Japan Sea. Bull Japan Sea Natl Fish Res Inst 43:69–81

Ikeda T, Hirakawa K, Imamura A (1992) Abundance, population structure and life cycle of a hyperiid amphipod *Themisto japonica* (Bovallius) in Toyama Bay, southern Japan Sea. Bull Plankton Soc Japan 39:1–16

Iriarte JL, González HE (2004) Phytoplankton size structure during and after the 1997/98 El Niño in a coastal upwelling area of the northern Humboldt Current System. Mar Ecol Prog Ser 269:83–90

Kimmel DG, Roman MR, Zhang X (2006) Spatial and temporal variability in factors affecting mesozooplankton dynamics in Chesapeake Bay: evidence from biomass size spectra. Limnol Oceanogr 51:131–141

Kobari T, Shinada A, Tsuda A (2003) Functional roles of interzonal migrating mesozooplankton in the western subarctic Pacific. Prog Oceanogr 57:279–298

Longhurst AR (1991) Role of the marine biosphere in the global carbon cycle. Limnol Oceanogr 36:1507–1526

Macpherson E, Gordoa A, Garcia-Rubies A (2002) Biomass size spectra in littoral fishes in protected and unprotected areas in the NW Mediterranean. Estuar Coast Shelf Sci 55:777–788

Marcolin CR, Schultes S, Jackson GA, Lopes RM (2013) Plankton and seston size spectra estimated by the LOPC and ZooScan in the Abrolhos Bank ecosystem (SE Atlantic). Cont Shelf Res 70:74–87

Matsuno K, Yamaguchi A (2010) Abundance and biomass of mesozooplankton along north-south transects (165°E and 165°W) in summer in the North Pacific: an analysis with an optical plankton counter. Plank Benthos Res 5:123–130

Matsuno K, Yamaguchi A, Imai I (2012) Biomass size spectra of mesozooplankton in the Chukchi Sea during the summers of 1991/1992 and 2007/2008: an analysis using optical plankton counter data. ICES J Mar Sci 69:1205–1217

Michaels AF, Silver MW (1988) Primary production, sinking fluxes and microbial food web. Deep-Sea Res 35A:473–490

Moore SK, Suthers IM (2006) Evaluation and correction of subresolved particles by the optical plankton counter in three Australian estuaries with pristine to highly modified catchments. J Geophys Res 111:C05S04, doi:10.1029/2005JC002920

Motoda S (1957) North Pacific standard net. Inform Bull Plank Japan 4:13–15 (in Japanese with English abstract)

Motoda S (1959) Devices of simple plankton apparatus. Mem Fac Fish Hokkaido Univ 7:73–94

Nakata K, Koyama S (2003) Interannual changes of the winter to early spring biomass and composition of mesozooplankton in the Kuroshio Region in relation to climatic factors. J Oceanogr 59:225–234

Nakata K, Koyama S, Matsukawa Y (2001) Interannual variation in spring biomass and gut content composition of copepods in the Kuroshio current, 1971–89. Fish Oceanogr 10:329–341

Napp JM, Ortner PB, Pieper RE, Holliday DV (1993) Biovolume-size spectra of epipelagic zooplankton using a multi-frequency acoustic profiling system (MAPS). Deep-Sea Res I 40:445–459

Nogueira E, Gonzárez-Nuevo G, Bode A, Varela M, Morán XAG, Valdés L (2004) Comparison of biomass and size spectra derived from optical plankton counter data and net samples: application to the assessment of mesoplankton distribution along the Northwest and North Iberian Shelf. ICES J Mar Sci 61:508–517

Odate K (1994) Zooplankton biomass and its long-term variation in the western North Pacific Ocean, Tohoku Sea Area, Japan. Bull Tohoku Natl Fish Res Inst 56:115–173 (in Japanese with English abstract)

Piontkovski SA, Williams R, Melnik TA (1995) Spatial heterogeneity, biomass and size structure of plankton of the Indian Ocean: some general trends. Mar Ecol Prog Ser 117:219–227

Quinones RA, Platt T, Rodriguez J (2003) Patterns of biomass-size spectra from oligotrophic waters of the Northwest Atlantic. Prog Oceanogr 57:405–427

Rodriguez J, Mullin MM (1986) Relation between biomass and body weight of plankton in a steady state oceanic ecosystem. Limnol Oceanogr 31:361–370

Schultes S, Sourisseau M, LeMasson E, Lunven M, Marié L (2013) Influence of physical forcing on mesozooplankton communities at the Ushant tidal front. J Mar Syst 109–110:S191–S202

Sheldon RW, Sutcliffe WH Jr, Paranjape M (1977) Structure of pelagic food chain and relationship between plankton and fish production. J Fish Res Bd Can 34:2344–2353

Shimode S, Toda T, Kikuchi T (2006) Spatio-temporal changes in diversity and community structure of planktonic copepods in Sagami Bay, Japan. Mar Biol 148:581–197

Shoden S, Ikeda T, Yamaguchi A (2005) Vertical distribution, population structure and life cycle of *Eucalanus bungii* (Copepoda: Calanoida) in the Oyashio region, with notes on its regional variations. Mar Biol 146:497–511
Sourisseau M, Carlotti F (2006) Spatial distribution of zooplankton size spectra on the French continental shelf of the Bay of Biscay during spring 2000 and 2001. J Geophys Res 111, doi: 10.1029/2005JC003063
Sprules WG, Munawar M (1986) Plankton size spectra in relation to ecosystem productivity, size and perturbation. Can J Fish Aquat Sci 43:1789–1794
Suthers IM, Taggart CT, Rissik D, Baird ME (2006) Day and night ichthyoplankton assemblages and zooplankton biomass size spectrum in a deep ocean island wake. Mar Ecol Prog Ser 322:225–238
Tarling GA, Stowasser G, Ward P, Poulton AJ, Zhou M, Venables HJ, McGill RAR, Murphy EJ (2012) Seasonal trophic structure of the Scotia Sea pelagic ecosystem considered through biomass spectra and stable isotope analysis. Deep-Sea Res II 59–60:222–236
Terazaki M (1993) Deep-sea adaptation of the epipelagic chaetognath *Sagitta elegans* in the Japan Sea. Mar Ecol Prog Ser 98:79–88
Van der Meeren T, Næss T (1993) How does cod (*Gadus morhua*) cope with variability in feeding conditions during early larval stage? Mar Biol 116:637–647
Volkov AF (2008) Mean annual characteristics of zooplankton in the sea of Okhotsk, Bering Sea and Northwestern Pacific (annual and seasonal biomass values and predominance). Russ J Mar Biol 34:437–451
Yamaguchi A, Matsuno K, Abe Y, Arima D, Ohgi K (2014) Seasonal changes in zooplankton abundance, biomass, size structure and dominant copepods in the Oyashio region analysed by an optical plankton counter. Deep-Sea Res I 91:115–124
Yasuda I (2003) Hydrographic structure and variability of the Kuroshio-Oyashio transition area. J Oceanogr 59:389–402
Yokoi Y, Yamaguchi A, Ikeda T (2008) Regional and interannual changes in the abundance, biomass and community structure of mesozooplankton in the western North Pacific in early summer; as analysed with an optical plankton counter. Bull Plank Soc Japan 55:79–88 (in Japanese with English abstract)
Zhou M (2006) What determines the slope of a plankton biomass spectrum? J Plankton Res 28:437–448
Zhou M, Huntley ME (1997) Population dynamics theory of plankton based on biomass spectra. Mar Ecol Prog Ser 159:61–73
Zhou M, Tande KS, Zhu Y, Basedow S (2009) Productivity, trophic levels and size spectra of zooplankton in northern Norwegian shelf regions. Deep-Sea Res II 56:1934–1944